Open-loop control of the wake behind a D-shaped bluff body

Li Yaqing[1], Bai Honglei[2] and Gao Nan[1*]

1. School of Aeronautics and Astronautics, Dalian University of Technology, Dalian, China
2. Dept. of Mechanical Engineering, University of Melbourne, Melbourne, Australia
* Corresponding author:gaonan@dlut.edu.cn

Abstract
Open-loop flow control method was used to affect the development of a turbulent wake behind a D-shaped bluff body. Loud speakers embedded inside the bluff body producing two zero-net-mass-flux jets through span-wise slots with a width of 2mm located along the upper and lower edges on the rear wall. Different excitation amplitudes and excitation frequencies were examined. Phase angles of 0 and 180 degrees between the velocity variations of the two jets were also compared. Smoke-wire visualization technique was used to visualize the evolutions of the large scale structures. It was found that when the ratio between the momentum of the actuating jets and the moment deficit caused by the bluff body (C_μ) was 0.1%, 5% drag reduction was achieved when the two jets excited in phase at a frequency of St_A=0.16, which was about 2/3 of the characteristic frequency of the natural wake structures. When the velocity of the two jets varied out of phase, no drag reduction was observed.

1. Introduction

Flow separation over a bluff body can be found in many applications. A shear layer grows on each side of the separation region. The large scale flow structures appear in the shear layer, they merge and grow in size [1]。 Effectively affect the development of the wake structures can reduce the form drag associated with the flow separation. Previous efforts on the control of the turbulent wake includes the using of passive methods and active control methods, recently reviewed by Choi et al.[2].

High frequency zero-net-mass-flux jet (or synthetic jet) actuator was widely used in the active control of separated flows. Compared with the passive control methods such as vortex generators, the active control methods have higher efficiency and better robustness. [3,4]. The periodic perturbations of the flow near the separation region promote the development of the large scale structures and enhance the momentum transport across the shear layer. The pressure on the solid surface, the trajectory of the shear layer and the size of the re-circulation region are changed. An array of several synthetic actuators was also used to control the separated flow. Bigger et al.[5] used an array of 6 zero-net-mass-flux jets distributed azimuthally around the edge of a disk to control the wake. They found the size of the separation region can be reduced as much as 10% when the actions of the actuators are in phase and the momentum ratio C_μ was 0.4%, 15% reduction in the separation length was found when helical actuation was used where the phase difference between the adjacent actuators was 60 degrees. Vukasinovic et al. [6] used an array of 11 actuators located azimuthally on a half circle around a hemisphere. They found when the excitation frequency was about 10 times of the natural shedding frequency (St_A=17.4~30.5), and the momentum ratio of the jets was 0.75%–2.3%, separation length was reduced significantly.

There are different arguments about the optimal actuation frequency in the literature. Amitay and Glezer[4] and Vukasinovic et al.[6] found that when the actuation frequency was more than 10 times of natural shedding frequency , St_A >10 St_o, when reducing the size of the separation bubble over a stalled wing was the prime target of the flow control. Yoshioka et al. [7,8] found actuation frequencies similar to the natural vortex shedding frequency of a separated flow over a back-ward facing step ($St_A \approx St_o$) were most effective in reducing the size of the separation bubble. Recently, Pastoor et al.[9] used open and close loop control methods to reduce the drag of a D-shaped body located in the center of a wind tunnel. The characteristics of the unforced wake downstream of a D-shaped body was well documented by Bearman[10] and the passive control of this flow using span-wise distributed vortex generators was studied by Park et al.[11]. There is a synthetic jet actuator along the upper and the lower edges of the rear surface of the D-shaped body used by

Pastoor et al.[9] and the velocity variations of the actuators were identical. They found when the actuation frequency was close to the natural shedding frequency of the turbulent wake $St_A = St_o = 0.24$, the drag was not reduced. The drag was reduced when the forcing frequency was smaller than the natural shedding frequency $0.1 < St_A < 0.2$. For the flow with a Reynolds number of 46000, when the actuation frequency was $St_A = 0.15$ and C_μ larger than 0.5%, the drag was reduced by approximately 15%. A D-shaped body similar to Pastoor et al. was used in the current investigation. The open loop control with momentum ratios C_μ less than 0.2% was examined here, where Pastoor et al.[9] only provided a few combinations of excitation amplitude and forcing frequency. Smoke-wire visualization technique was also used to study the effect of harmonic excitations on the development of the large scale flow structures. The experimental methodologies will be presented in the next section, followed by the results and the summaries.

2. Experimental setup and methods

A 63mm height, 280mm wide D-shaped body made from Acrylic was mounted in a open-loop suction-type wind tunnel with a 300mm x 300mm x 700mm test section, shown in figure 1(a). The wind tunnel has a contraction ratio of 9 and a turbulence intensity of 0.5% in the test section. The D-shaped body was similar to the one used by Pastoor et al.[9]. The length, height and width of the D-shaped body were 188.5mm × 285mm × 63mm(L, W, H), respectively. Two arrays of 4.5W loud-speakers (three in each array, positioned side by side in the span-wise direction) were used to form two slot jets through a 3.5 high cavity and a 165mm long (in z direction) 2mm wide slot. The speakers have a diameter of 45mm and a resistance of 8 ohms. The jets were directed at 45 degrees to the free-stream. Sinusoidal signals from a signal generator

$$g_1(t)=A\sin(2\pi f_A t) \text{ and } g_2(t)=A\sin(2\pi f_A t+\phi)$$

were amplified using TDA7492 amplifiers and applied to the top and bottom speaker arrays, respectively. Here, ϕ is the phase difference between the two signals, f_A is the forcing frequency and A was the forcing amplitude. A Hanghua CTA hot-wire anemometer and a probe with 4.5 micron diameter tungsten wire were used to characterize the jet velocity at 1mm downstream of the center of the jet, as shown in figure 1(b). Typical transients of the jet velocity were shown in figure 2. The strength of the actuation were characterized using the momentum ratio

$$C_\mu=2(s/H)(u^2_A/U^2_{\infty,c}).$$

Here, u_A is the root-mean-square value of the jet velocity measured at the jet exit, s is the width of the slot. There are two jets on the D-shaped body, thus the momentum of the jets were multiplied by a factor of 2.

The D-shaped body was supported by two aluminum square bars located at 123.5mm downstream of the leading edge(or x=-165mm) and z=±135mm. The bars also served as force transducers with strain gauges attached to the center of the bars. The bars were drilled with equally spaced 2.4mm holes at the locations above and below the strain gauges to minimize the drag caused by the supporting bars. Signals from the strain gauges were amplified using a amplifier with a gain of 100.

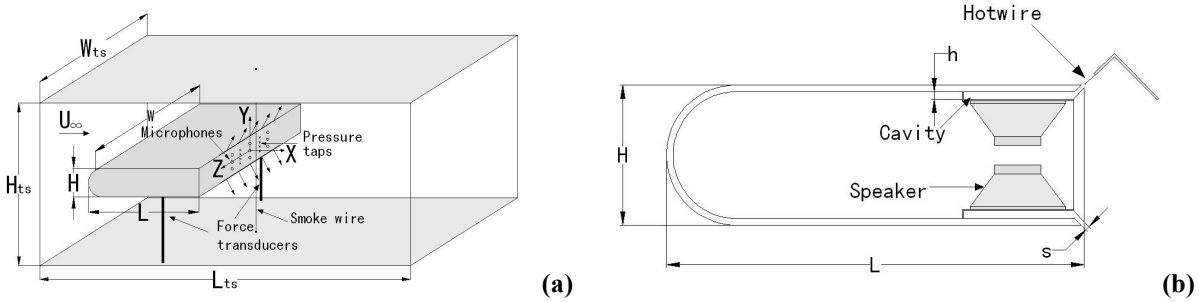

Figure. 1 Schematic of (a) the test section and (b) D-shaped body in an open-loop suction type wind tunnel

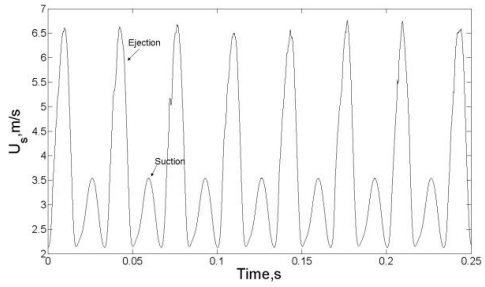

Figure 2. Typical transient velocity measured at the exit of the synthetic jet for a forcing frequency of f_A=30Hz and a forcing amplitude of A=0.11V.

Measurements were performed with an free-stream velocity (U_∞) of 9.24m/s, the blockage ratio of the test section was 21%, the incoming velocity was adjusted to $U_{\infty,c}$=11.7m/s using a method given in [9]. The Reynolds number and the Strouhal number are given by

$$Re_H=U_{\infty,c}\,H/\nu \text{ and } St=f\,H/U_{\infty,c}.$$

All the measurements and visualizations were performed with Re=47000. Here in this paper, x is the stream-wise direction, y is the vertical direction and z is the span-wise direction.

There are two columns (z/H=±0.44) and 4 rows (y/H=±0.08, ±0.24) of 1mm diameter pressure taps were mounted on the rear wall of the bluff body. Each pressure tap was connected to a CYH-130 pressure transducer using 0.8mm inner diameter flexible tubing to measure the mean static pressure on the rear wall. The pressure transducer was calibrated using a YJB-2500 water manometer with a resolution of 0.1Pa.

The signals from the force transducers, the pressure transducer and the hot-wire anemometer were acquired using a NI-6014 DAQ card and Labview routines. The sampling frequency was 2048Hz and sampling time was 150s. The static pressure of the rear wall of the D-shaped body and the side wall of the wind tunnel ΔP and the drag were presented using non-dimensional coefficients

$$C_P=\frac{\Delta P}{\rho U_{\infty,c}^2/2} \quad \text{and} \quad C_D=\frac{F}{\rho U_{\infty,c}^2 HW/2}, \text{ respectively.}$$

The measurements uncertainties of C_P and C_D are ±2% and ±2.5%, respectively. C_P and C_D for different forcing frequencies (St_A<0.33) and amplitudes (Cμ<0.4%) were examined.

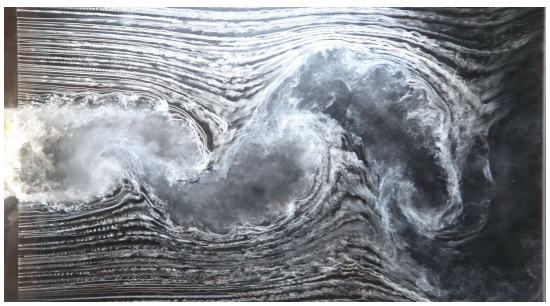

Figure 3. Smoke-wire visualization of a turbulent wake behind a D-type bluff body without excitations.


(a)
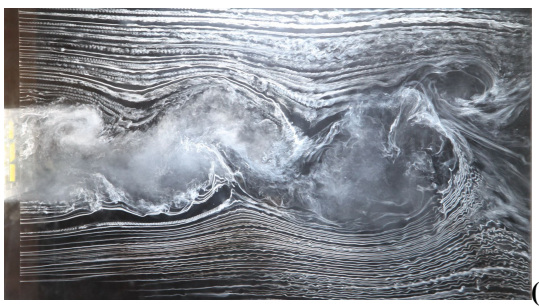
(b)

Figure 4. Smoke-wire visualization of a turbulent wake behind a D-type body under in-phase excitation of C_μ=0.1% and (a) St_A=0.16 and (b) St_A=0.24.

Smoke-wire visualization technique was used to study the evolution of the flow structures. A 304 stainless steel wire with a diameter of 0.1mm was stretched vertically at 5mm downstream of the rear surface of the bluff body along in the central plane of the tunnel (x/H=0.08, z=0). The metal wire was connected to two 2200μF capacitors using aluminum electrodes and heavy gauge wires. The capacitors discharged high current electricity through the metal wire and heated up liquid droplets attached to the wire producing smoke streaks. A short amount of time after the start of discharging, a triggering signal was send to the camera and the flash light to record the streak-lines. The actions were controlled by a circuit with an Atmega16 single chip computer. The discharge voltage of the capacitor was set to 75V and the time delay between the discharging and the shutter triggering signal was 0.01s in the current investigation. Mixture of paraffin and diesel was applied to the wire using a brush. A Canon 5D Mk-II camera with a Canon Speedlite 600EX flash light was used to record the image. The far side wall of the wind tunnel was painted with candle-soot paint to increase the quality of the pictures.

3. Results and Discussions

3.1 Baseline flow

The smoke-wire visualization image of the baseline flow (the unforced flow) with a Reynolds number of 47000 in figure 3 showed that a separation region formed downstream of the D-shaped body. Large scale alternating structures formed downstream of the body and grew in size. Fourier transform of the instantaneous forces indicated that the Strouhal number of the unforced wake ($St_o = f_oH/U_{\infty,c}$) was 0.25. The drag coefficient C_{Do} was 0.57 and the averaged static wall pressure coefficient $<C_{Po}>$ was -0.51. $<C_{Po}>$ agreed with the measurements by Pastoor et al. [9] and Bearman[10]. The boundary layer thickness measured near the rear wall (x/H=0.01, z/H=0) was 10.8mm (δ/H=0.171), similar to Pastoor et al. [9].

3.2 In-phase excitations

Two different phase angles between the velocities of the upper and the lower synthetic jets (ϕ=0 and π) were examined. The flow visualization images for the case with in-phase (ϕ=0) actuators actions at a frequency of St_A of 0.16 and 0.24 are shown in Figure 4. When St_A was 0.16 (approximately 2/3 of the natural shedding frequency), the alternating flow structures was not visible in wake. Countering rotating large scale structures were generated in pairs at the same time and they traveled downstream with a similar velocity. The wake in the flow with the paired structures seemed to be smaller in the vertical direction than the flow with the alternating flow structures. When the flow was forced with St_A of 0.24, the counter rotating structures were initially paired near the trailing edge of the bluff body, but the paired structures seemed to be unstable, the structures appeared to have different traveling velocities and the flow soon became similar to alternating structures of unforced wake at a location away from the bluff body.

The drag and static pressure on the rear wall of the bluff body for a fixed forcing amplitude C_μ of 0.1% and St_A less than 0.33 were shown in figure 5. The drag was reduced when the forcing frequency St_A was less than 0.22. The maximum drag reduction of 5% occurred at St_A of 0.16, suggesting the smaller wake size in y direction caused by the in-phase forcing can be related to the drag reduction. The drag became larger than the natural flow when the forcing frequency St_A was larger than 0.22, particularly at the natural shedding frequency St_A=0.24, the drag increased for approximately 18%. High frequency forcing seemed to promote the transition of the paired structures to the alternating wake structures, and increase the drag.

The drag and static pressure coefficients on the rear wall for a fixed forcing frequency St_A of 0.16 and different forcing amplitudes (C_μ) less than 0.2% are shown in figure 6, the results by Pastoor et al.[9] for a similar flow are also shown for comparisons. Drag was increased when C_μ was less than 0.04%, particularly at C_μ=0.01% where the drag increased for nearly 8%. The mechanism causing the drag to increase at small C_μ was not clear and needs further investigations. Drag was reduced when C_μ was more than 0.06%, the drag reduction was more than those found by Pastoor et al.[9].

The drag and static pressure coefficients on the rear wall for a forcing frequency St_A of 0.24 and forcing amplitudes C_μ less than 0.44% are shown in figure 7. Drag was increased when C_μ was less than 0.2%, particularly when C_μ was around 0.1% where the drag increases for as much as 13%. The drag appeared to be independent of the forcing when the forcing amplitude was further increased to $C_\mu > 0.2\%$.

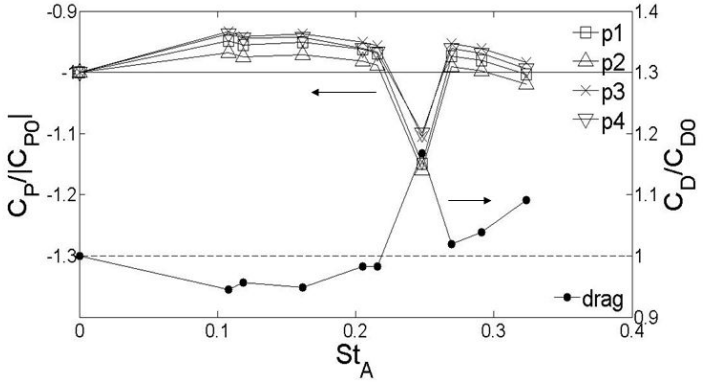

Figure. 5 Distributions of the drag and pressure coefficients for in-phase excitation by the upper and lower slot jets for flow with Re_H=47000, C_μ=0.1%, C_{Po} and C_{Do} are the drag and pressure coefficients when there was no excitation. The pressure taps p1 to p4 were located at x=0, z=0.44H and y=0.24H, 0.08H, -0.08H, -0.24H, respectively.

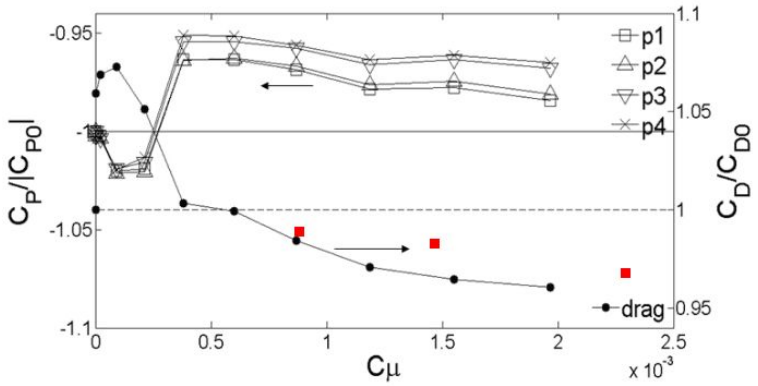

Figure. 6 Distributions of the drag and pressure coefficients for in-phase excitation by the upper and lower slot jets for different forcing amplitude for flow with St_A=0.16 and different momentum ratios. Red squares are the results by Pastoor et al.[9]

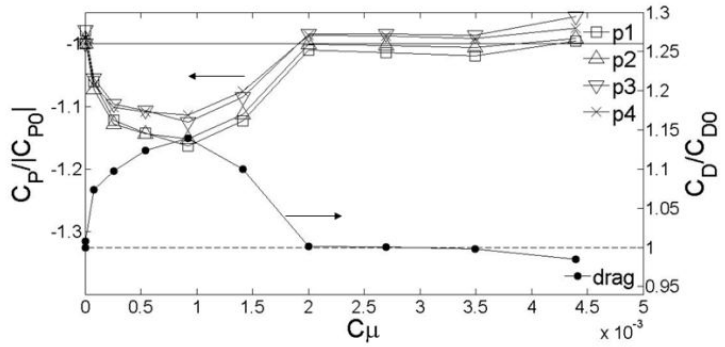

Figure. 7 Distributions of the drag and pressure coefficients for in-phase excitation by the upper and lower slot jets for different forcing amplitude for flow with St_A=0.24.

3.3 Anti-phase excitations

When the actions of the two actuators were 180 degrees out of phase, strong alternating structures formed in the wake, especially in the flow forced at a frequency of the natural shedding frequency (St_A=0.24), shown in figure 8. The vertical growth rate of the flow with anti-phase excitations appeared to be much larger than the natural wake or the in-phase excited flows, the drag was also larger than the natural flow at all the forcing frequencies, as shown in figure 9. The drag was increased as much as 25% when the flow was forced at the natural shedding frequency.

The effect of forcing amplitude on the drag when the flow was forced at St_A = 0.24 is shown in figure 10. The drag became larger than that of the natural flow for all the forcing amplitudes studied here. The drag increased quickly with C_μ when C_μ was less than 0.05%, the drag was less sensitive to C_μ when C_μ was larger than 0.05%.

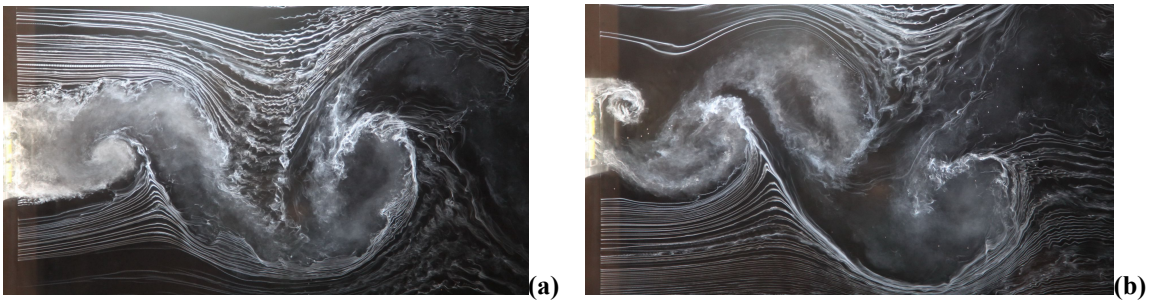

Figure.8 Smoke-wire visualization of a turbulent wake behind a D-type body under anti-phase excitation of C_μ=0.1% and (a) St_A=0.16 and (b) St_A=0.24.

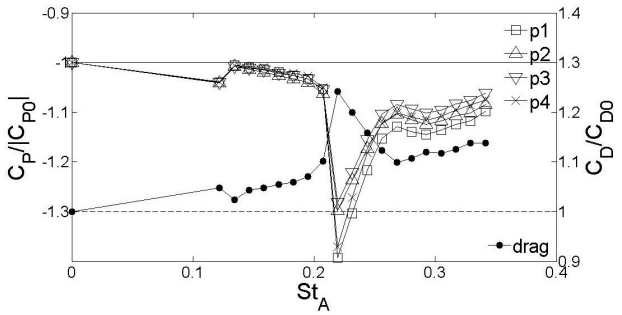

Figure. 9 Distributions of the drag and pressure coefficients for anti-phase excitation by the upper and lower slot jets for flow with Re_H=47000, C_μ=0.001.

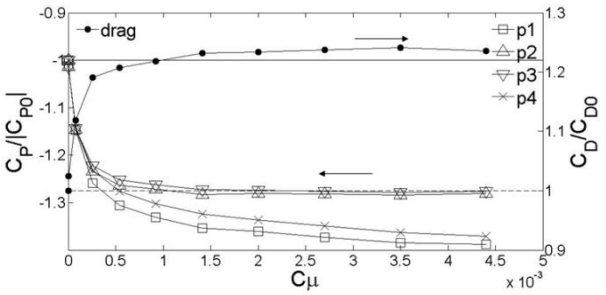

Figure. 10 Distributions of the drag and pressure coefficients for anti-phase excitation by the upper and lower slot jets for flow with St_A=0.24 and different momentum ratios.

4. Conclusions

Wake behind a D-shaped body with a Reynolds number of 47000 was forced using a pair of zero-net-mass-flux jets directed at a 45 degree to the free-stream in the upper and lower corners of the trailing surface of the D-shaped body with different frequencies (St_A = 0–0.35) and amplitudes (C_μ = 0–0.2% for the in-phase excitation, C_μ = 0–0.44% for the anti-phase excitations). A maximum 5% force reduction was achieved when the actions of the actuators were in-phase at a momentum ratio C_μ of 0.1% and St_A of 0.16 which was approximately 2/3 of the natural shedding frequency. Smoke wire visualization study revealed that the drag reduction was caused by the suppression of the vortex shedding by the paired counter-rotating structures generated by the in-phase forcing. When the forcing frequency was increased to St_A=0.24, the paired structures were not stable, the flow soon transitioned to a state similar to the natural wake, the drag was also more than that of the natural flow. The results also showed that when the actuators were anti-phase, the drag increased for all the forcing amplitudes, but the drag was more sensitive to the forcing when C_μ was less than 0.05%, drag did not change much when C_μ further increased. Close-loop control with various control methods will be studied using this facility in the future.

Acknowledgements
The work was supported by 973 plan (2014CB744100), State Key Laboratory of Aerodynamics (SKLA20130102) and Dalian University of Technology (DUT14LK07).

References

[1]. Williamson, C.H.K. and R. Govardhan, Vortex-induced vibrations. Annual Review of Fluid Mechanics, 2004. 36: p. 413-456.
[2]. Choi, H., W.-P. Jeon, and J. Kim, Control of flow over a bluff body. Annual Review of Fluid Mechanics, 2008. 40: p. 113-139.
[3]. Cattafesta L.N. and M. Sheplak, Actuators for active flow control. Annual Review of Fluid Mechanics, 2011. 43: p. 247-272.
[4]. Amitay, M. and A. Glezer, Aerodynamic flow control using synthetic jet actuators, in Control of Fluid Flow P. Koumoutsakos and I. Mezic, Editors. 2006, Springer: Berlin. p. 45-73.
[5]. Bigger, R.P., H. Higuchi, and J.W. Hall, Open-loop control of disk wakes. AIAA Journal, 2009. 47(5): p. 1186-1194.
[6]. Vukasinovic, B., D. Brzozowski, and A. Glezer, Fluidic control of separation over a hemispherical turret. 2009. 47: p. 2212-2222.
[7]. Yoshioka, S., S. Obi, and S. Masuda, Turbulence statistics of periodically perturbed separated flow over backward-facing step. International Journal of Heat and Fluid Flow, 2001. 22: p. 393-401.
[8]. Yoshioka, S., S. Obi, and S. Masuda, Organized vortex motion in periodically perturbed turbulent separated flow over a backward-facing step. International Journal of Heat and Fluid Flow, 2001. 22: p. 301-307.
[9]. Pastoor, M., et al., Feedback shear layer control for bluff body drag reduction. Journal of Fluid Mechanics, 2008. 608: p. 161–196.
[10]. Bearman, P.W., Investigation of the flow behind a two-dimensional model with a blunt trailing edge and fitted with splitter plates. Journal of Fluid Mechanics, 1965. 21: p. 241-256.
[11]. Park, H., et al., Drag reduction in flow over a two-dimensional bluff body with a blunt trailing edge using a new passive device. Journal of Fluid Mechanics, 2006. 563: p. 389-314.